



Observing the simulation behaviour of Magnesium alloy metal sandwich panel under cyclic loadings

M. S. Baharin, S. Abdullah

Department of Mechanical and Manufacturing Engineering, Faculty of Engineering and Built Environment, Universiti Kebangsaan Malaysia, 43600 UKM Bangi, Selangor, Malaysia
mbsbshamsul@gmail.com, shabrum@ukm.edu.my

N. Md Nor

Civil Engineering Studies, Universiti Teknologi MARA, Kawangan Pulau Pinang, 13500 Permatang Pauh, Pulau Pinang, Malaysia
ida_nsn@uitm.edu.my

M. K. Faidzi, A. Arifin, S. S. K. Singh

Department of Mechanical and Manufacturing Engineering, Faculty of Engineering and Built Environment, Universiti Kebangsaan Malaysia, 43600 UKM Bangi, Selangor, Malaysia
khairul.faidzi@gmail.com, azli@ukm.edu.my, salvinder@ukm.edu.my

ABSTRACT. This study aims to investigate the delamination effect of a metal sandwich panel using a four-point bending simulation under continual spectrum loading. The most recent core designs of the sandwich panel have a cavity that can increase vulnerability in terms of bonding strength under constant cyclic loading. The sandwich panel is simulated under constant cyclic loading using different core design configurations, which are rounded dimple, hemispherical dimple, and smooth surface core design. There are two types of conditions used; no pre-stress and pre-stress loads with variable stress ratios based on Gerber stress life theory. Results showed that dimple core design enhanced mechanical behaviour and fatigue life performance about 33% and 5%, respectively, compared to the sandwich panel with a smooth surface core design. It is highlighted that modification on the surface of core design could be beneficial to enhance the bonding strength performance of sandwich panels and prevent early delamination under extreme conditions such as constant cyclic loading. This study is beneficial to enhance the bonding strength for sandwich panels against extreme conditions such as high impact load and continuous cyclic load.

KEYWORDS. Computational analysis; Cyclic loading; Fatigue life; Magnesium alloy; Sandwich panel.



Citation: Baharin, M. S., Abdullah, S., Md Nor, N., Faidzi, M. K., Arifin, A., Singh, S. S. K., Evaluating metal sandwich panel with mg alloy as core under constant cyclic stress with simulation approach, Frattura ed Integrità Strutturale, 61 (2022) 230-243.

Received: 14.02.2022

Accepted: 04.04.2022

Online first: 24.05.2022

Published: 01.07.2022

Copyright: © 2022 This is an open-access article under the terms of the CC-BY 4.0, which permits unrestricted use, distribution, and reproduction in any medium, provided the original author and source are credited.



INTRODUCTION

Over the last few decades, researchers have studied sandwich panels with different parameters such as using honeycomb core, the number of core layers used, and their fatigue behaviour and applications [1–4]. Wang et al.'s studies of sandwich panels in industries where each kilogramme of materials costs a lot of money, sandwich panels have become one of the most efficient ways to achieve the highest bending stiffness and strength-to-weight ratios in structural components [5]. They are made of two thin, rigid, high-strength facing skins linked by a thick, light core attached using a strong structural adhesive, capable of transmitting loads [6]. Instead of traditional materials like steel and aluminium, hybrid material structures have been considered by the automotive industry [7] in sandwich panel applications as they will enhance their mechanical performance. The use of lightweight core, for example, Mg alloy, to separate the facing skins will also increase the moment of inertia with minimal increase of weight resulting in a structure that can withstand stresses [8]. The combination of magnesium alloy and steel is gaining popularity among the metal combination concept because magnesium alloy density is much lower at 1.35-1.85 g/cm³, about two-thirds than aluminium alloy density or a third of steel density [9,10]. Compared to other conventional structural materials like steel and aluminium, magnesium has a lesser corrosion resistance [11] and viability [12,13].

For sandwich panels, however, failures like delamination are likely to occur due to poor transverse tensile and interlaminar shear strengths in comparison to their in-plane qualities while also developing internal delamination damage but not evident to the human eye [14]. To create a functioning and safe structure, it is crucial to identify delamination on the sandwich panel as it will also be the reason for the composite materials' rigidity and to reduce long-term performance [14,15]. Although many components possess elastic cycle stress, plastic deformations are caused by stress concentration resulting in a loss in fatigue life.

Therefore, this study focuses on the mechanical behaviour of a laminated composite plate made of AR500 steel (face sheets), epoxy, and AZ31B magnesium alloy (main core) using four-point bending under constant cyclic loading on three sandwich panels designated as SP-1, SP-2, and SP-3. SP-1 is a sandwich panel with a rounded dimple. SP-2 is a sandwich panel with a hemispherical dimple on the surface of the magnesium alloy core while the surface of the magnesium alloy core for SP-3 is a solid core. Since the computational approaches based on the finite element method (FEM) have been exclusively used for the past few years to simulate the mechanical behaviour of a structure [16] and compare computational results with experiments [10,17], computational analysis was used in this study to simulate the geometrical sandwich panel and modelled under static and fatigue life theories under constant stress conditions to assess fatigue behaviour of the proposed sandwich panel with various stress ratios. This computational analysis facilitated a considerable early identification of delamination processes encountered by the three-dimensional geometrical metal sandwich panel. It showed the importance of core design when the behaviour of delamination was observed at the bonding area of the sandwich panel and how total deformation and stress distribution were related to the fatigue life assessment.

MATERIALS AND METHODS

The whole experiment was simulated and the default material parameters in the finite element software programme database were chosen, such as Young's modulus, Poisson ratio, shear modulus, yield strength, tensile strength, and elongation for AR500 steel, AZ31B magnesium alloy [18,19], and epoxy resin and hardener [20]. Fig. 1 shows the process flow of the sandwich panel simulation in this study. With the help of finite element modelling software, a geometrical model of a metal sandwich panel was created. The numbers of elements and nodes for SP-1 were 45418 and 103419, SP-2 were 15156 and 54227, and SP-3 were 10164 and 56795 with the boundary condition of four-point bending under loading condition with and without pre-stress with variable stress ratios. As shown in Fig 1, the Gerber's mean stress correction was used instead of Goodman or Soderbeg because during the experiment, it served as a marker for the area below the point of failure based on the Gerber's parabola line to determine the lowest fatigue life limit possible [21] and it was also suitable for ductile materials [22]. Besides, the negative mean stress was not bound by both Soderberg and Goodman's mean stress theories [22] which made it unsuitable for this study due to the use of negative mean stress in the fatigue analysis.

As illustrated in Fig. 2, each plate is designed as a three-dimensional model and assembled to make a single-piece composite model that made up of AR500, magnesium alloy and epoxy. The epoxy adhesive is 1 mm. The total thickness is 25 mm, excluding the adhesive, following the standard similar to the body panel of a lightweight armour vehicle based on previous studies [10,23]. They were later simulated as a four-point bending test in the finite element analysis software. The designs



of SP-1, SP-2, and SP-3 are shown in Tab. 1, Fig. 3, and Fig. 4 with dimensions based on previous studies [13]. Based on Fig. 4, the diameter is 6 mm to match the 3 mm depth with SP-1.

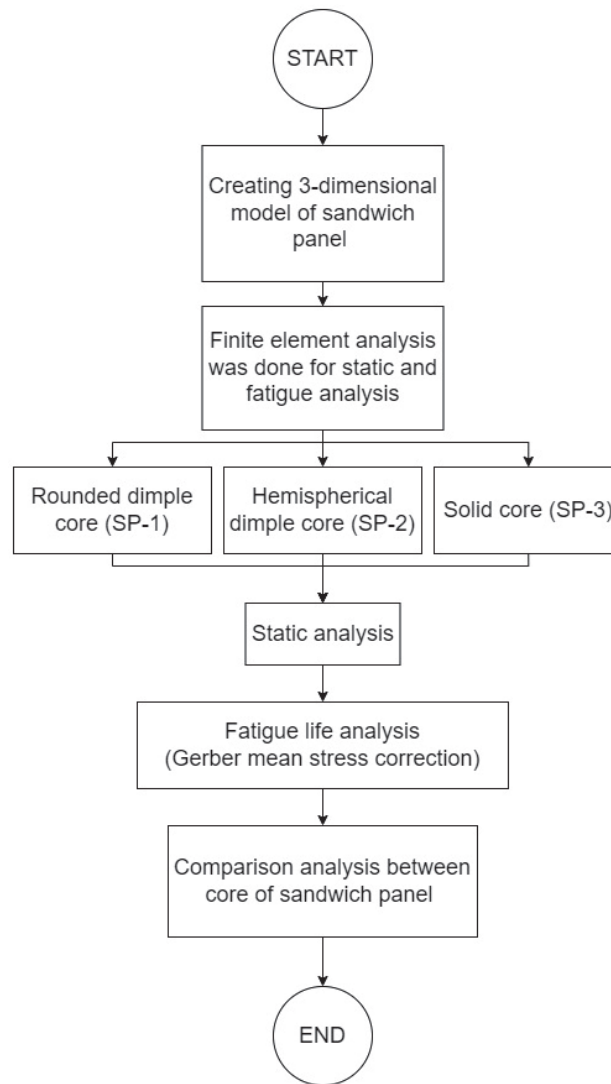


Figure 1: The process flow fatigue life stress distribution and deformation of sandwich panel.

Core arrangement	Plate dimension (h × w), mm	Dimple thickness, mm	Dimple diameter, mm
AR500-Rounded dimple core-AR500 [SP-1]	180 × 40	3	10
AR500-Hemispherical dimple core-AR500 [SP-2]	180 × 40	3	6
AR500-Solid core-AR500 [SP-3]	180 × 40	-	-

Table 1: Configuration of a sandwich panel for simulation.

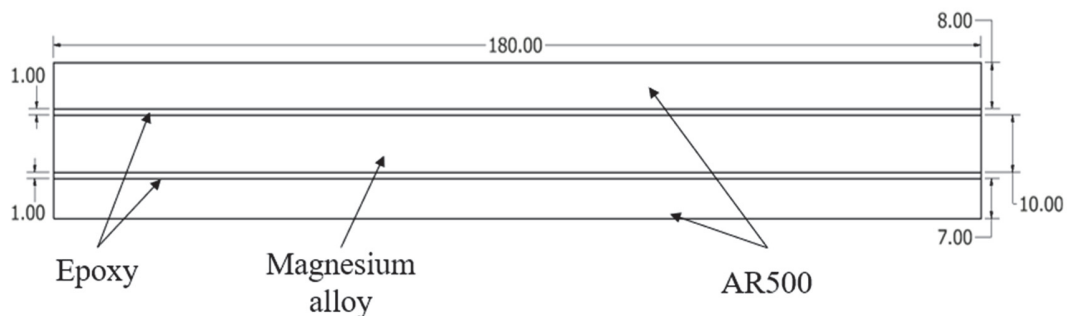


Figure 2: A 2-dimensional view of geometrical sandwich panel, dimension in mm.

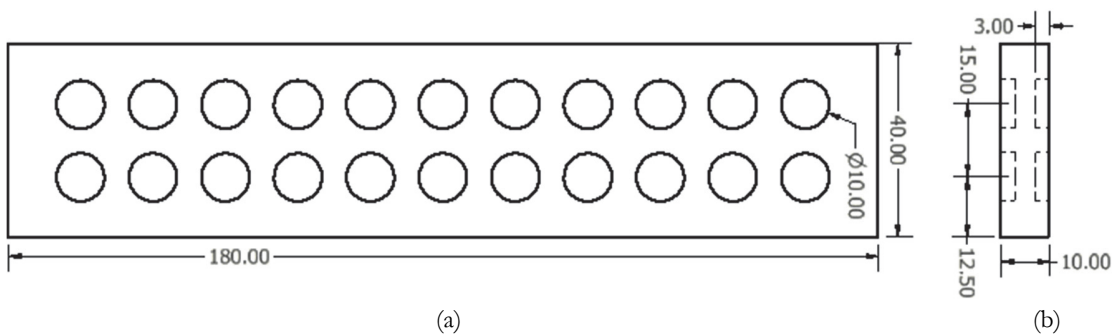


Figure 3: Details for SP-1 a) top view b) side view, dimension in mm.

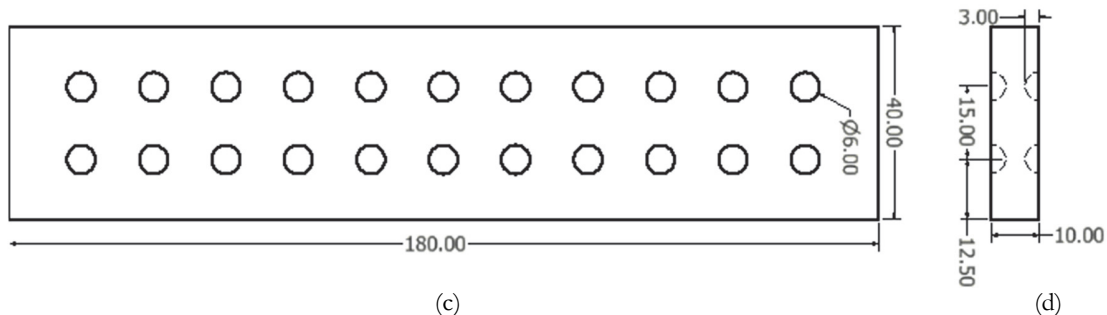


Figure 4: Details for SP-2 a) top view b) side view, dimension in mm.

Static load analysis

For the static load experiment, stress distribution (von Mises stress) and total deformation [24] results for the whole body and bonding area of the panel were analysed. The sandwich panel's loading was chosen based on the percentage of AZ31B magnesium alloy's yield strength, 165 MPa [19], varying at 60%, 70%, 75%, 80%, and 90%. This assures the sandwich panel's safety since magnesium alloy has a lower yield strength value than AR500 steel. If the percentage of AR500 steel yield strength was used in this simulation, the structure would fail since the core was made of magnesium alloy.

Fatigue life analysis

The geometrical sandwich panel was subjected to a constant amplitude loading for fatigue life analysis to observe fatigue behaviour and life analysis for all sandwich panels. Furthermore, the four-point bending was simulated with and without pre-stresses based on the loading data history. The fatigue life performance of all sandwich panels was determined by this pre-conditioning and allowed for stress relief and early panel failure owing to residual stress after the panel was loaded. In this simulation, the fatigue strength factor was set to default, assuming that the material's surfaces had no contamination and polished perfectly. The fatigue performance was compared to the total deformation and stress distribution experienced by all sandwich panels to identify the delamination mechanism and its correlations in contributing to failure under static and continual repeated loading. 10 Hz of loading frequency was applied to the four-point bending test simulation with and without pre-stresses at different stress ratios. With pre-stress, the σ_{max} values employed were -0.2, -0.4, -0.6, and -0.8. The



σ_{min} value was still -1 resulting in stress ratio, R, value to vary at $R = 5$, $R=2.5$, $R=1.67$, and $R=1.25$. For the four-point bending test without pre-stress, the values of σ_{min} were -0.2, -0.4, -0.6, and -0.8, and $\sigma_{max} = 0$ for the maximum value while R was infinity. The load was applied without being stressed beforehand. Eqn. (1) shows how the R is calculated with this formula in the study [25]:

$$R = \frac{\sigma_{min}}{\sigma_{max}} = \frac{-1}{-0.8} = 1.25 \quad (1)$$

RESULTS AND DISCUSSION

The results of the four-point bending simulation performed using a finite element software tool were examined under static and fatigue conditions. The performance of the metal sandwich panel was calculated for static analysis based on the stress distribution and total deformation experienced by the sandwich panel's bonding area. To assess the behaviour and strength of the metal sandwich panels under static loading, the two factors in the static analysis (stress distribution and deformation) were crucial to identify the effects of the core surface configuration on the performance of metal sandwich panels.

As for the cyclic loading, once applied and simulated on the sandwich panel, the conditions stated earlier were critical to encourage the stress release condition and prevent failure due to stress residual on the panel.

Static analysis

Each sandwich panel's von Mises stress distribution and total deformation data exhibited a nearly identical trend, but with varied maximum and lowest values as the magnesium, alloy core had different kinds of design configurations. According to Fig. 5, SP-1 has a maximum von Mises stress distribution difference in the bonding area of over 39.12%, while SP-2 is 30% with SP-3 at both the lowest load (32076 N) and greatest load (48114 N). The first maximum deformation difference between SP-1 and SP-3 at both lowest and highest load is over 16.25%, while SP-2 is over 3.14%. Based on the percentage difference of all the geometrical model, sandwich panel that has dimple which are SP-1 and SP-2 performs better than solid core, SP-3 because it can withstand higher von Mises stress at the bonding region. This means that structural integrity of the panel was increased.

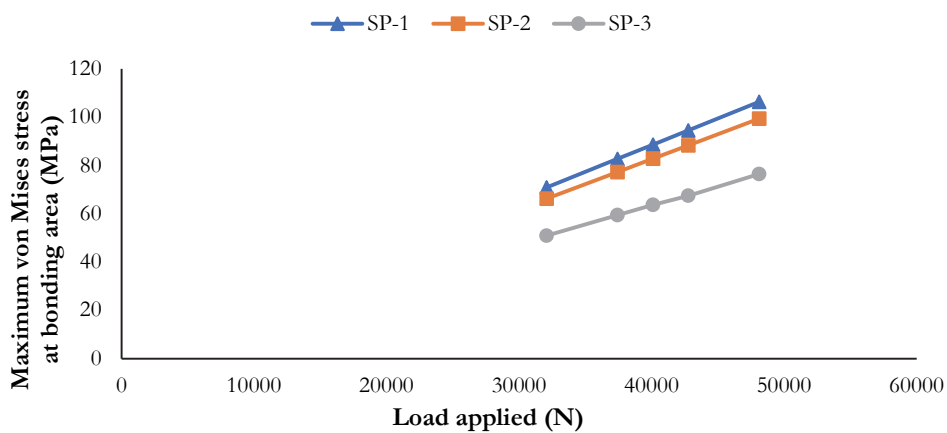


Figure 5: Maximum von Mises distribution at bonding area against loading given for SP-1, SP-2, and SP-3

As shown in Fig. 6, the overall deformation of the sandwich panels at the bonding area follows a similar pattern. When compared to SP-3, an increase in maximum deformation for each load provided can be deduced. The decline in core density in the dimple area contributed to the increase in maximum deformation. Even though the greatest stress distribution was possessed by SP-1, SP-2 owned the least deformation with 0.221 mm, still greater compared to SP-3 (0.214 mm) ever so slightly due to the presence of dimples in SP-1 and SP-2 [13].

The von Mises stress distribution for SP-1 at bonding area was 88.623 MPa at maximum and 0.294 MPa at minimum values based on Fig. 7. The delamination phenomenon is shown by the contour distribution at the bonding area. The findings indicate that SP-1 and SP-2 perform 32.73% and 26.09%, respectively, better in terms of decreasing delamination risk at the

sandwich panel's bonding layer than SP-3. The simulation proves that the presence of dimples on the surface cores in SP-1 and SP-2 has enhanced the structural integrity [26] of the panel compared to solid core design because it can withstand larger amount of stress on bonding region.

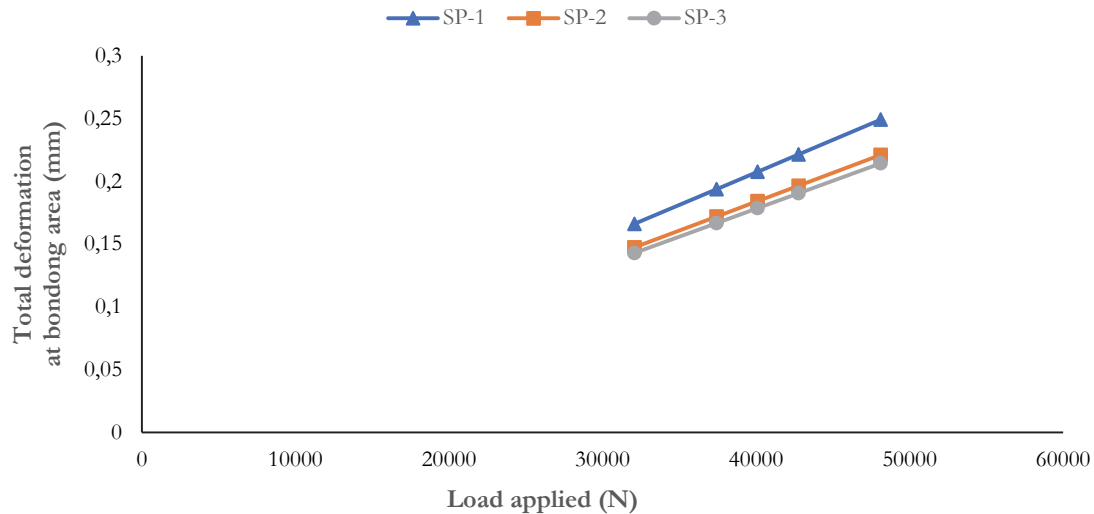


Figure 6: Total deformation (bond area) against loading given for SP-1, SP-2, and SP-3 at the bonding area

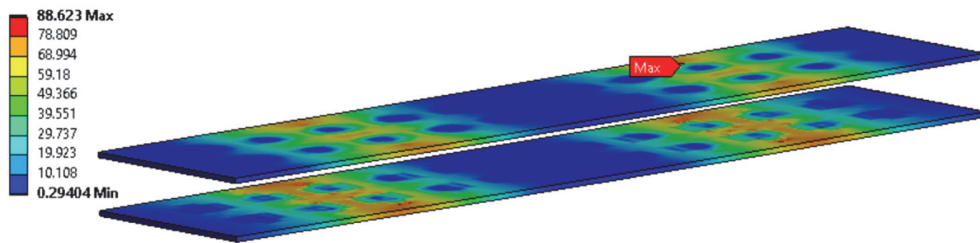


Figure 7: Simulation result of von Mises stress distribution for SP-1 with 40095 N of load at the bonding area

Fatigue life analysis with pre-stress

In Fig. 8, average fatigue life values for all sandwich panels are compared using the lowest stress ratio of 1.25 between SP-3 and SP-1 first, then the comparison between SP-3 and SP-2. The percentage difference of average fatigue life between SP-3 and SP-1 was 0.998% when the first load of 32076 N was applied. The difference increased to 2.76% when the final load of 48114 N was applied. The percentage difference of average fatigue life between SP-3 and SP-2 was 0.744% at the lowest load of 32076 N. The average fatigue life increased to 1.73% at the greatest load of 48114 N. SP-1 produced the highest average fatigue life of 18698.6 compared to SP-2 (1879.2). SP-3 had the lowest fatigue life value of 1847 with $R = 1.25$ and the highest loading of 48114 N. Since both comparisons showed that SP-1 and SP-2 had better fatigue life than SP-3, it proved that the presence of dimple enhanced sandwich panel performance [26]. The coefficient of determination (R^2) reflected the variance in response to the average fatigue life and load applied as presented in Fig. 8. The statistic in the regression was used to measure the degree of fit of a model. The R^2 value indicated how accurate the model matched the data produced [27] and it ranged between 0 and 1. To interpret the relationship between the two variables, the average fatigue life, and load applied, the higher R^2 (close to 1) meant that the result was better and more reliable [28]. Based on Fig. 8, the simulation results are considered reliable because R^2 value for all sandwich panel is close to 1. Compared to R^2 value of SP-2 and SP-3 which is 0.79 and 0.94, respectively, SP-1 simulation has the best results with R^2 equal to 1.

When $R = 1.25$ and a load of 37422 N were applied, the fatigue life distribution over the whole geometrical sandwich panel and at the bonding area can be observed in Fig. 9. The difference was pretty large when focusing on the contour trend on the fatigue life study with pre-stress. Based on Fig. 9, although the overall fatigue life of the sandwich panel is high, the bonding area has a significant chunk of red contour trend at the point where stress is applied as shown in Fig. 9 (b), indicating a low fatigue value. When $R = 1.25$, the red contour indicates a severe delamination phenomenon. Due to the presence of



a pre-stress state before loading, the fatigue life becomes more severe, which agrees to a study made by Elmushyaki [29] on a structure that exhibits greater damage when preloaded force is given.

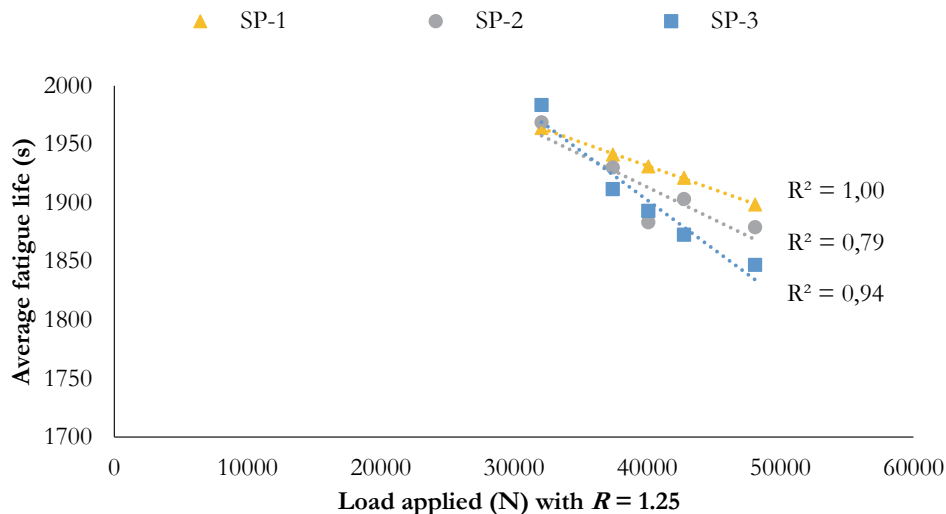


Figure 8: Average fatigue life against given load for all three metal sandwich panels at stress ratio, $R = 1.25$

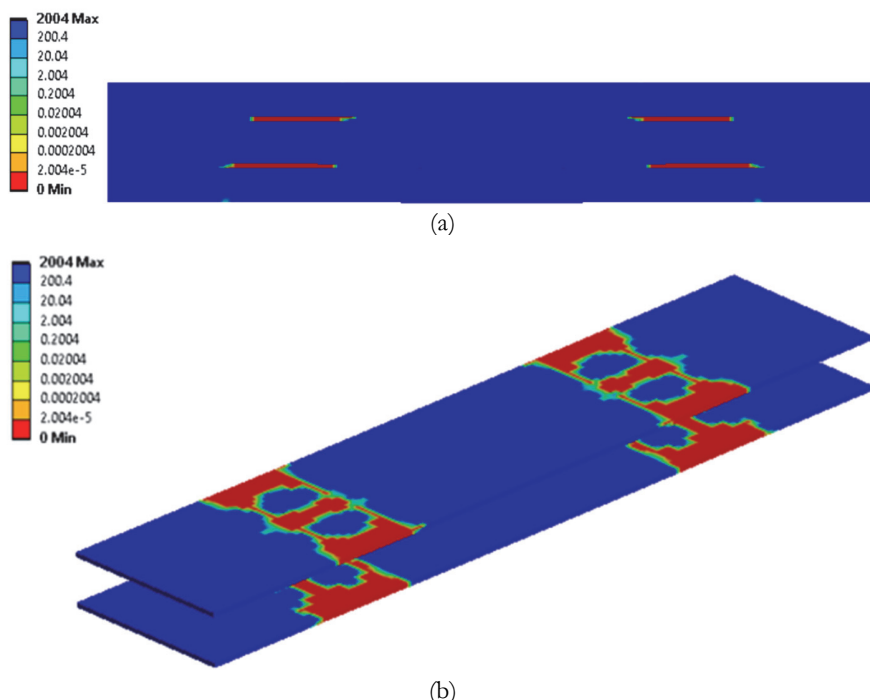


Figure 9: Fatigue life distribution modelled using finite element to determine the critical region based on; (a) front view of sandwich panel geometrical body, (b) bonding area for SP-1 at stress ratio, $R = 1.25$ with a load of 37422N.

At the greatest stress ratio with $R = 5$, Fig. 10 shows a comparison of average fatigue life values for all sandwich panels with three different core surface designs. Comparisons were made between SP-3 and SP-1 followed by SP-3 and SP-2. At a load of 32076 N, 0.166% was the difference and increased to 4.97% for the final load of 48114 N. As for the comparison between SP-3 and SP-2, it was 0.16% at the starting load of 32076 N and the differences grew to a value of 3.29% with the final load of 48114 N. It was found that SP-1 had the highest fatigue life value with an average value of 1821.7 when comparison was made between all three core design sandwich panels at the highest stress ratio of $R = 5$. SP-2 had the second highest value of 1783.3 seconds, and SP-3 obtained the lowest fatigue life value of 1733.3 seconds. Based on Fig. 10, the simulation results

for all the test were considered reliable since R^2 value are more than 0.80 and close to 1. However, SP-1 and SP-3 has the best simulation results because R^2 equal to 0.99 compared to SP-2 with $R^2 = 0.86$.

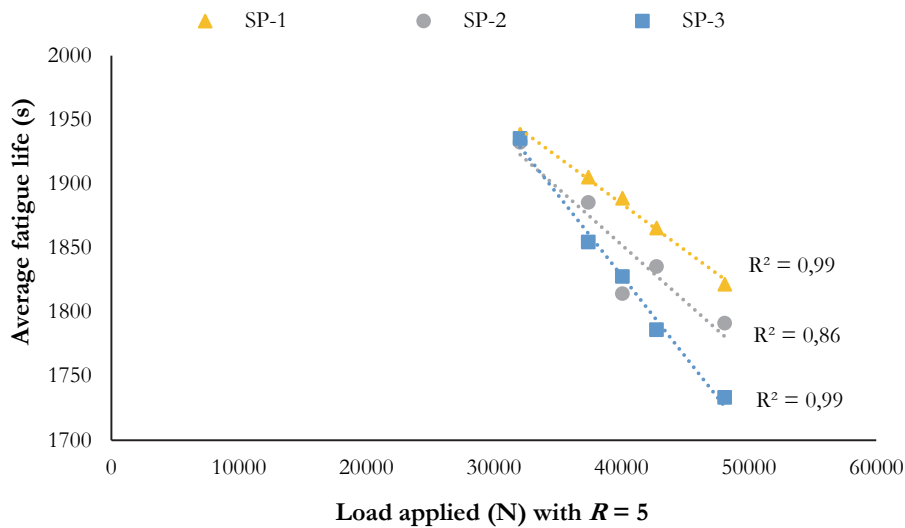


Figure 10: Average fatigue life against given load for all three metal sandwich panels at stress ratio, $R = 5$.

When $R = 5$, the fatigue life distribution across the geometrical sandwich panel and at the bonding area is shown in Fig. 11. The degree of failure for the sandwich panel under continual cyclic loading was related to the increment of stress ratio by comparing the contour trend at $R = 1.25$ (Fig. 8). The red colour contour in Fig. 11 (a) and (b), which is the critical region, indicated 0 fatigue life, which means the material failed in that area followed by debonding between the layers of the sandwich panel (delamination) [13]. The effect was visible at the bonding location, as illustrated in Fig. 11 (b) by the trend of the fatigue contour. It affected that particular area because of the force given at that point due to the concept of four-point bending test.

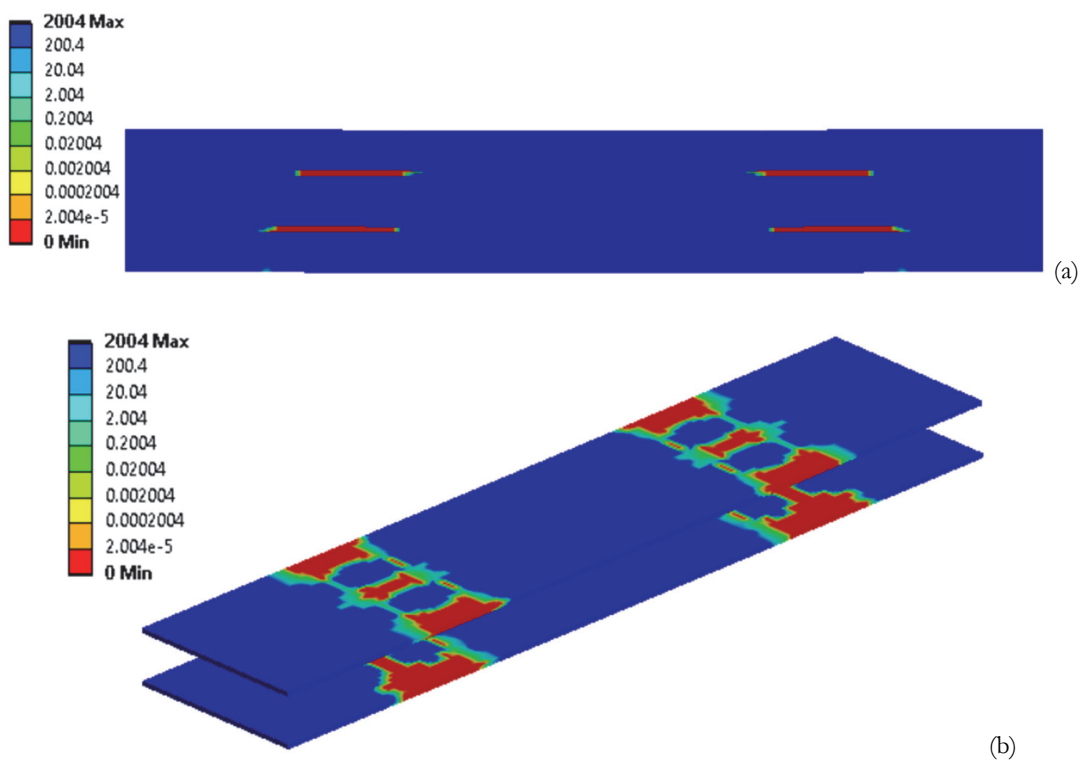


Figure 11: Fatigue life distribution modelled using finite element to determine the critical region based on; (a) front view of sandwich panel geometrical body, (b) bonding area for SP-1 at stress ratio, $R = 5$ with a load of 37422N



Fatigue life analysis without pre-stress

Even though the value obtained from the sandwich panel with various Mg alloy core designs had identical patterns, the highest and lowest averages of fatigue life for all three differed from one another and the four-point bending test was without pre-stress. The comparison of the average fatigue life differences was made between SP-1, SP-2, and SP-3 as shown in Fig. 12. The first part of the comparison was the percentage difference between SP-3 and SP-1. No differences were found at 32076 N but increased to 4.97% for the final load of 48114 N. As for the comparison between SP-3 and SP-2, there were no differences between them with a load of 32076 N and the disparity grew to 0.025% of the difference in average fatigue life with the final load of 48114 N. Since both comparisons showed that SP-1 and SP-2 had better fatigue life than SP-3, proving the presence of dimple enhanced sandwich panel performance [13]. Based on Fig. 11, the simulation results for all the test were considered reliable since R^2 value are close to 1. However, SP-1 has the best simulation results since R^2 equal to 0.80 which is closest to 1 as compared to SP-2 and SP-3 with $R^2 = 0.73$ and $R^2 = 0.74$.

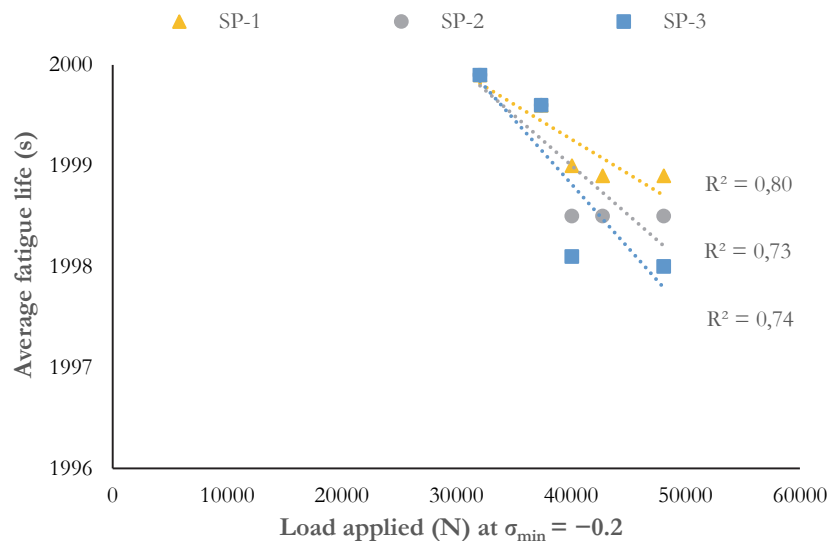


Figure 12: Average fatigue life against given load for SP-1, SP-2, and SP-3 at $\sigma_{min} = -0.2$.

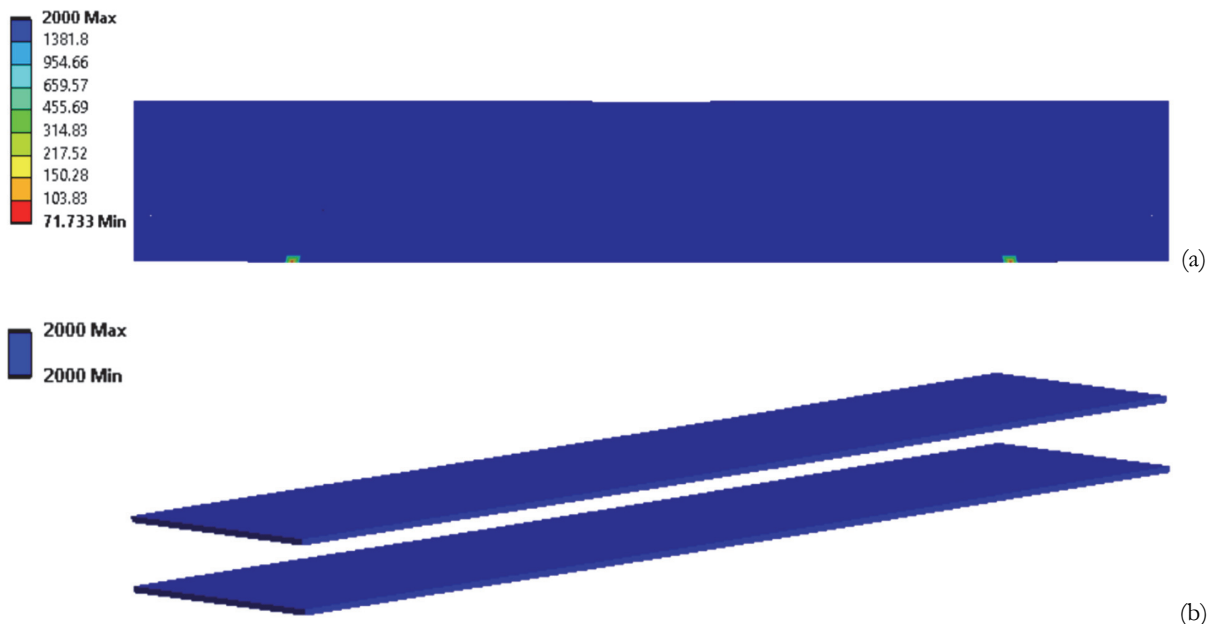


Figure 13: Fatigue life distribution modelled using finite element to determine the critical region based on; (a) front view of sandwich panel geometrical body, (b) bonding area for SP-2 at $\sigma_{min} = -0.2$ with a load of 37422N

The fatigue life distribution across the geometrical sandwich panel structure and at its bonding demonstrated no failure indication when $\sigma_{min} = -0.2$, as shown in Fig. 13. The majority of the contour trend was blue, indicating that the sandwich panel's fatigue life was 2000 cycles before failing with the lowest minimum value of life at 71 cycles at the skin's surface of AR 500, which means the results agreed with the previous study [29] on how preloaded force exhibited greater damage on structure and vice versa.

Based on Fig. 14, comparisons of the average fatigue life were carried out between SP-1, SP-2, and SP-3 with $\sigma_{min} = -0.8$. The first part of the comparison was the percentage differences of average fatigue life between SP-3 and SP-1, which was 0.194% at 32076 N followed by 0.332% of the difference with 37422 N of load. It exhibited a 0.810% difference in average fatigue life value at 40095 N load. There was an increase of percentage difference to 2.71% at 42768 N but decreased to 2.56% for the final load of 48114 N. As for the comparison between SP-3 and SP-2, it was 0.347% at the starting load of 32076 N. Next, it had a difference of 0.259% with a load of 37422 N. It had a difference of 0.332% at 40095 N of load and when the load increased to 42768 N, the disparity grew to 1.69%. However, the percentage difference decreased to 0.995% of average fatigue life with the final load of 48114 N. Based on Fig. 14, it can be concluded that SP-1 and SP-2 had better fatigue life than SP-3, proving the presence of dimple enhanced sandwich panel performance [26]. Since the R^2 value for each sandwich panel in Fig. 14 is higher than 0.8, the simulation results for all the test were considered reliable. However, the best simulation results are SP-1 with $R^2 = 1$ as compared to R^2 value for SP-2 and SP-3 which is 0.99 and 0.94, respectively.

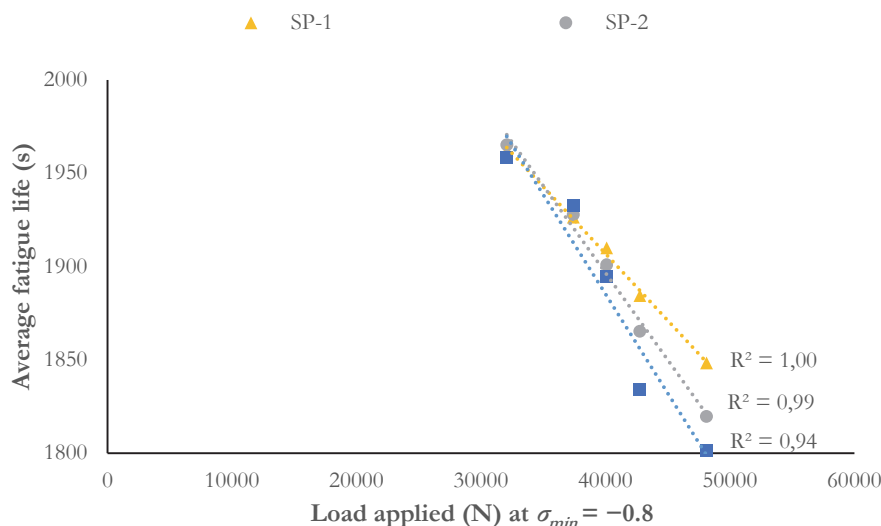


Figure 14: Average fatigue life with given load for all three metal sandwich panels at $\sigma_{min} = -0.8$

When $\sigma_{min} = -0.8$, the fatigue life distribution across the geometrical sandwich panel and at the bonding area is visible, as shown in Fig. 15. The majority of the contour colours were blue and lighter hues of blue when stress was applied, indicating the geometrical sandwich panel's maximum fatigue life. A very tiny section of the bonding region indicated a minimum value of fatigue life [17]. The results were different from Figs. 12 and 13 due to different values of minimum stress amplitude, σ_{min} used in the stress ratio calculation which can be referred to Eqn. (1)[3]. The σ_{min} used for simulation in Fig. 14 is higher than σ_{min} used for simulation in Fig. 12 which cause the reduction of sandwich panel fatigue life as showed in Figs. 14 and 15.

Further issues on the failure trend under both static and cyclic simulations

Based on the trend analysis of the sandwich panel thoroughly explained in Figs. 5 to 15, it was discovered that the mechanical performance and fatigue failure of sandwich panels can be accelerated by surface modification and material type and this has also been discussed by Faidzi et al. [26]. This study focused on evaluating three types of magnesium alloy with various core designs joined by steel and produced a distinct sandwich panel performance that gave various von Mises stress distribution, permanent deformation, and average fatigue life. It was feasible to make a sandwich panel out of non-homogeneous materials [10] even though the majority of sandwich panels were made of homogeneous material [13,30]. The principle was nearly equivalent to the use of a honeycomb composite structure, which reduces the laminated composite structure mass while still providing high special stiffness, special strength, and durability [16].



Furthermore, Palomba et al. [31] had also investigated the collapse response of an aluminium honeycomb sandwich panel under fatigue bending and discovered that the span spacing affected the deformation mode owing to skin tension. The core shearing was a prominent failure mechanism. It has been demonstrated that core structures with a large cavity area carried out in the present study were prone to collapsing and deforming, which impacted the bonding integrity of sandwich panels. It has been enhanced by Beden et al. [21], stating that surfaces had a great influence on the fatigue behaviour of a material, as well as the situation of this study which compared three surfaces of magnesium alloy plate designs the stress value of von Mises, deformation, and the average fatigue life of varying averages.

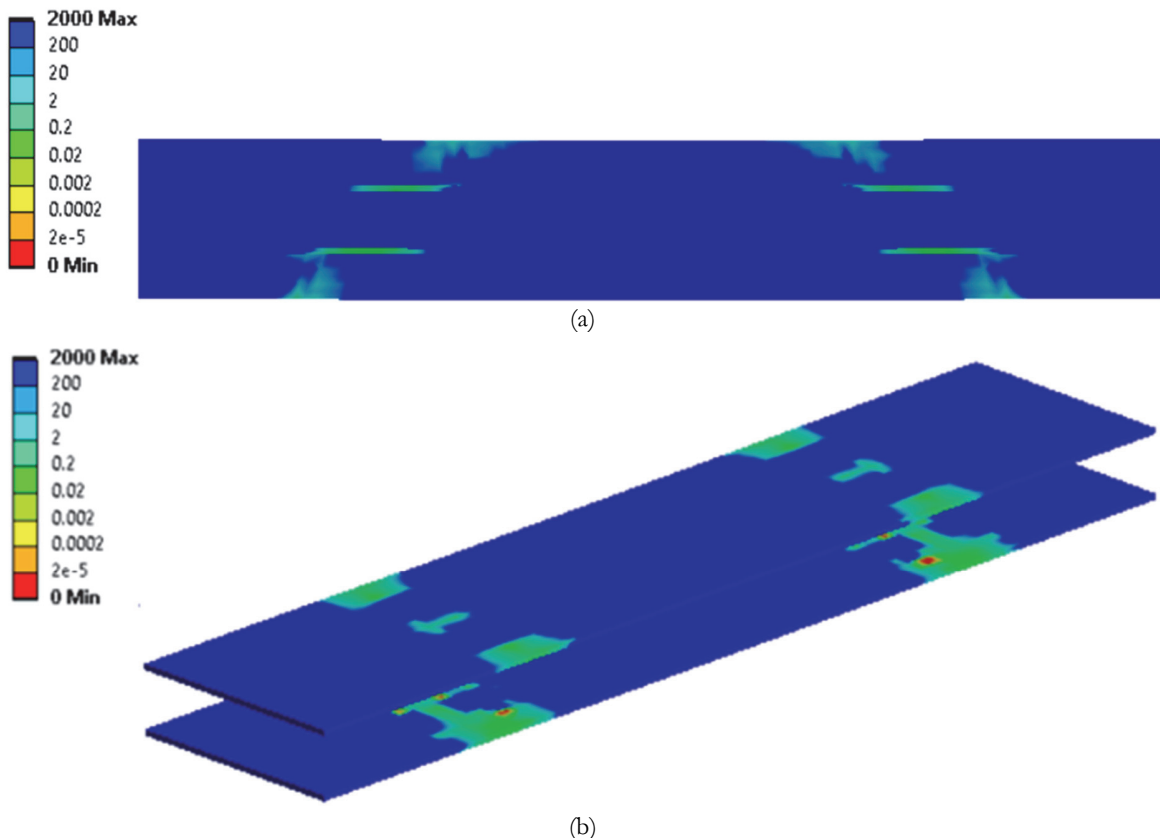


Figure 15: Fatigue life distribution modelled using finite element to determine the critical region based on; (a) front view of sandwich panel geometrical body, (b) bonding area for SP-1 at $\sigma_{min} = -0.8$ with a load of 37422N

CONCLUSION

The results of this investigation show that the toughness and stress strength of a sandwich panel is boosted by the presence of a dimple. Both SP-1 and SP-2 demonstrate similar trends in this study at the bonding region of a non-homogenous sandwich panel which possesses a greater distribution of von Mises stress. Even though the dimpled core design has a minor increase for permanent deformation compared to the smooth core surface, deformation is less than 30% under static load which is within an acceptable limit. The average fatigue lifetime values for SP-2 and SP-3 are almost identical at the highest stress ratio of 5 and highest loading of 48114 N (1821.7 and 1783.3 – both with pre-stress), which is superior to SP-1 (1733.3 – with pre-stress). The data prove that sandwich panel's mechanical performance improves by the presence of dimple on the surface core while the delamination phenomenon that occurs on the bonding area can be minimised by introducing a dimple design on the core because it offers a larger surface area for the adhesive material to connect non-homogeneous sandwich panel materials which indirectly reduce the overall weight. Finally, without integrating a sophisticated failure modelling, the study recommends detection analysis for early delamination with the computational technique for three-dimensional sandwich panels.



ACKNOWLEDGEMENT

The authors would like to acknowledge the computational facilities support provided by Universiti Kebangsaan Malaysia

FUNDING

This research was funded by Universiti Kebangsaan Malaysia (GUP-2021-016).

T

CONFLICTS OF INTEREST

The authors declare no conflict of interest.

T

AUTHOR CONTRIBUTIONS

The following contributions to this work were made by the following authors - Conceptualization, S.Abdullah, M.S.Baharin; Investigation, M.S.Baharin, M.K.Faidzi, and S.Abdullah; Resources, S.Abdullah, and A.Arifin; Supervision, S.Abdullah; Software, S.S.K Singh; Writing-Original Draft Preparation, M.S.Baharin, S.Abdullah; Writing-Review and Editing, S.Abdullah, N. Md Nor.

DATA AVAILABILITY STATEMENT

The processed data/material required to reproduce these findings cannot be shared at this time as the data also form part of an ongoing study.

REFERENCE

- [1] Wang, J., Shi, C., Yang, N., Sun, H., Liu, Y., Song, B. (2018). Strength, stiffness, and panel peeling strength of carbon fiber-reinforced composite sandwich structures with aluminum honeycomb cores for vehicle body, Compos. Struct., 184, pp. 1189–1196, DOI: 10.1016/j.compstruct.2017.10.038.
- [2] Palomba, G., Epasto, G., Crupi, V., Guglielmino, E. (2018). Single and double-layer honeycomb sandwich panels under impact loading, Int. J. Impact Eng., 121, pp. 77–90, DOI: 10.1016/j.ijimpeng.2018.07.013.
- [3] Ma, M., Yao, W., Jiang, W., Jin, W., Chen, Y., Li, P. (2020). Fatigue Behavior of Composite Sandwich Panels Under Three Point Bending Load, Polym. Test., 91, pp. 106795, DOI: 10.1016/j.polymertesting.2020.106795.
- [4] Castanie, B., Bouvet, C., Ginot, M. (2020). Review of composite sandwich structure in aeronautic applications, Compos. Part C Open Access, 1, pp. 100004, DOI: 10.1016/j.jcomc.2020.100004.
- [5] Wang, Z. (2019). Recent advances in novel metallic honeycomb structure, Compos. Part B Eng., 166, pp. 731–741, DOI: 10.1016/j.compositesb.2019.02.011.
- [6] Faidzi, M.K., Abdullah, S., Abdullah, M.F., Azman, A.H., Hui, D., Singh, S.S.K. (2021). Review of current trends for metal-based sandwich panel: Failure mechanisms and their contribution factors, Eng. Fail. Anal., 123, pp. 105302, DOI: 10.1016/j.englfailanal.2021.105302.
- [7] Vignesh, N.J., Hynes, N.R.J. (2018). Thermal analysis of friction riveting of dissimilar materials, AIP Conf. Proc., 1953,



- pp. 2022, DOI: 10.1063/1.5033285.
- [8] Sun, G., Chen, D., Wang, H., Hazell, P.J., Li, Q. (2018). High-velocity impact behaviour of aluminium honeycomb sandwich panels with different structural configurations, *Int. J. Impact Eng.*, 122, pp. 119–136, DOI: 10.1016/j.ijimpeng.2018.08.007.
- [9] Apelfeld, A., Krit, B., Ludin, V., Morozova, N., Vladimirov, B., Wu, R.Z. (2017). The characterization of plasma electrolytic oxidation coatings on AZ41 magnesium alloy, *Surf. Coatings Technol.*, 322, pp. 127–133, DOI: 10.1016/j.surfcoat.2017.05.048.
- [10] Rahman, N.A., Abdullah, S., Abdullah, M.F., Zamri, W.F.H., Omar, M.Z., Sajuri, Z. (2018). Experimental and numerical investigation on the layering configuration effect to the laminated aluminium/steel panel subjected to high speed impact test, *Metals (Basel.)*, 8(9), DOI: 10.3390/met8090732.
- [11] Jin, H., Javaid, A. (2020). A new cladding technology to bond aluminium on magnesium, *Mater. Sci. Technol. (United Kingdom)*, 36(10), pp. 1037–1043, DOI: 10.1080/02670836.2020.1747186.
- [12] Abdullah, M.F., Abdullah, S., Rahman, N.A., Risby, M.S., Omar, M.Z., Sajuri, Z. (2016). Improvement of high velocity impact performance of carbon nanotube and lead reinforced magnesium alloy, *Int. J. Automot. Mech. Eng.*, 13(2), pp. 3423–3433, DOI: 10.15282/ijame.13.2.2016.11.0283.
- [13] Faidzi, M.K., Abdullah, S., Abdullah, M.F., Singh, S.S.K., Azman, A.H. (2021). Evaluating an adhesive effect on core surface configuration for sandwich panel with peel simulation approach, *J. Mech. Sci. Technol.*, 35(6), pp. 2431–2439, DOI: 10.1007/s12206-021-0514-3.
- [14] Tian, Z., Yu, L., Leckey, C. (2015). Delamination detection and quantification on laminated composite structures with Lamb waves and wavenumber analysis, *J. Intell. Mater. Syst. Struct.*, 26(13), pp. 1723–1738, DOI: 10.1177/1045389X14557506.
- [15] Fotouhi, M., Saeedifar, M., Sadeghi, S., Ahmadi Najafabadi, M., Minak, G. (2015). Investigation of the damage mechanisms for mode I delamination growth in foam core sandwich composites using acoustic emission, *Struct. Heal. Monit.*, 14(3), pp. 265–280, DOI: 10.1177/1475921714568403.
- [16] Amulani, A., Pratap, H., Thomas, B. (2021). Investigation of static and fatigue behavior of honeycomb sandwich structure: a computational approach, *J. Brazilian Soc. Mech. Sci. Eng.*, 43(11), pp. 2022, DOI: 10.1007/s40430-021-03195-y.
- [17] Hussain, M., Khan, R., Abbas, N. (2019). Experimental and computational studies on honeycomb sandwich structures under static and fatigue bending load, *J. King Saud Univ. - Sci.*, 31(2), pp. 222–229, DOI: 10.1016/j.jksus.2018.05.012.
- [18] Borrisutthekul, R., Miyashita, Y., Mutoh, Y. (2005). Dissimilar material laser welding between magnesium alloy AZ31B and aluminum alloy A5052-O, *Sci. Technol. Adv. Mater.*, 6(2), pp. 199–204, DOI: 10.1016/j.stam.2004.11.014.
- [19] Feng, F., Huang, S., Meng, Z., Hu, J., Lei, Y., Zhou, M., Yang, Z. (2014). A constitutive and fracture model for AZ31B magnesium alloy in the tensile state, *Mater. Sci. Eng. A*, 594, pp. 334–43, DOI: 10.1016/j.msea.2013.11.008.
- [20] Abdullah, S., Abdullah, M.F., Jamil, W.N.M. (2020). Ballistic performance of the steel-aluminium metal laminate panel for armoured vehicle, *J. Mech. Eng. Sci.*, 14(1), pp. 6452–6460, DOI: 10.15282/jmes.14.1.2020.20.0505.
- [21] Beden, S.M., Abdullah, S., Ariffin, A.K., Al-Asady, N.A., Rahman, M.M. (2009). Fatigue life assessment of different steel-based shell materials under variable amplitude loading, *Eur. J. Sci. Res.*, 29(2), pp. 157–169.
- [22] Bader, Q., Kadum, E. (2014). Mean stress correction effects on the fatigue life behavior of steel alloys by using stress life approach theories, *Int. J. Eng. Technol. IJET-IJENS*, 14(04).
- [23] Rahman, N.A., Abdullah, S., Abdullah, M.F., Omar, M.Z., Sajuri, Z., Zamri, W.F.H. (2018). Ballistic limit of laminated panels with different joining materials subjected to steel-hardened core projectile, *Int. J. Integr. Eng.*, 10(5), pp. 8–14, DOI: 10.30880/ije.2018.10.05.002.
- [24] Upreti, S., Singh, V.K., Kamal, S.K., Jain, A., Dixit, A. (2019). Modelling and analysis of honeycomb sandwich structure using finite element method, *Mater. Today Proc.*, 25, pp. 620–625, DOI: 10.1016/j.matpr.2019.07.377.
- [25] Zakaria, K.A., Abdullah, S., Ghazali, M.J. (2016). A Review of the loading sequence effects on the fatigue life behaviour of metallic materials, *J. Eng. Sci. Technol. Rev.*, 9(5), pp. 189–200, DOI: 10.25103/jestr.095.30.
- [26] Faidzi, M.K., Abdullah, S., Abdullah, M.F., Azman, A.H., Singh, S.S.K., Hui, D. (2021). Computational analysis on the different core configurations for metal sandwich panel under high velocity impact, *Soft Comput.*, 25(16), pp. 10561–10574, DOI: 10.1007/s00500-021-06015-6.
- [27] Akossou, A.Y.J. (2013). Impact of data structure on the estimators R-square and adjusted R-square in linear regression., *Int. J. Math. Comput.*
- [28] Kasuya, E. (2019). On the use of r and r squared in correlation and regression, *Ecol. Res.*, 34(1), pp. 235–236, DOI: 10.1111/1440-1703.1011.
- [29] Elmushyakhi, A. (2019). Collapse mechanisms of out-of-plane preload composite sandwich beams under in-plane



- loading, J. Build. Eng., 26, pp. 100875, DOI: 10.1016/j.jobe.2019.100875.
- [30] Lee, W.G., Kim, J.S., Sun, S.J., Lim, J.Y. (2018). The next generation material for lightweight railway car body structures: Magnesium alloys, Proc. Inst. Mech. Eng. Part F J. Rail Rapid Transit, 232(1), pp. 25–42, DOI: 10.1177/0954409716646140.
- [31] Palomba, G., Crupi, V., Epasto, G. (2019). Collapse modes of aluminium honeycomb sandwich structures under fatigue bending loading, Thin-Walled Struct., 145, pp. 2022, DOI: 10.1016/j.tws.2019.106363.